

Fingering instability of a suspension film spreading on a spinning disk

Mayuresh Kulkarni,¹ Subhadarshinee Sahoo,¹ Pankaj Doshi,^{1, a)} and Ashish V. Orpe^{1, b)}
Chemical Engineering Division, CSIR-National Chemical Laboratory, Pune 411008, India

The spreading of a thin film of suspension on a spinning disk and the accompanying contact line instability is studied through flow visualization experiments. The critical radius for the onset of instability shows an increase with increase in the particle fraction (ϕ_p) before decreasing slightly at the highest value of ϕ_p studied, while the instability wavelength (λ) exhibits a non-monotonic dependence. The value of λ is close to that for a partially wetting liquid at lower ϕ_p , it decreases with increasing ϕ_p to a minimum before increasing again at largest ϕ_p . The non-monotonic trends observed for λ are discussed in light of the linear stability analysis of thin film equations derived for suspensions by Cook *et al.* [Linear stability of particle-laden thin films, *Eur. Phys. J.: Spec. Top.* **166**, 77 (2009)] and Balmforth *et al.* [Surface tension driven fingering of a viscoplastic film, *J. Non Newtonian Fluid Mech.* **142**, 143 (2007)]

I. INTRODUCTION

The spreading of a thin, viscous, film of liquid under external forcing (gravity or centrifugal) comprises of two regions: a flat region, the dynamics of which are determined by the balance between driving force and viscous dissipation and a second region near the advancing front, the shape of which is governed by the interplay between the liquid surface tension and the driving force. This second region, termed capillary ridge, is susceptible to perturbations in the transverse direction eventually growing as fingers.^{1–8} The presence of particles in such a spreading thin film of liquid (i.e., a suspension or a slurry) is encountered in different applications^{9–11} and can exhibit several complexities during spreading and ensuing fingering patterns.^{12–14}

For suspensions which exhibit yield stress behavior, the capillary ridge gets stabilized by the innate yield strength of the fluid allowing the film to spread to a larger area before the instability ensues.^{12,15} Linear stability analysis of the thin film equations for such yield stress fluids, incorporating a suitable stress constitutive equation, correctly predicts the observed behavior.¹⁵ In certain cases, however, the instability can be simply due to local yielding of the suspension¹⁴ and not the usual contact line instability along the advancing film front. An enhancement in the fingering instability, compared to the base suspending liquid, is predicted using linear stability analysis of thin film equations for hard sphere, non-Brownian, well-mixed suspensions.¹⁶ This enhancement is found to be slightly subdued for the case of settling, heavier particles, also observed in experiments.¹³

Here, we report interesting and novel experimental observations on a thin film of suspension spreading on a horizontal spinning disk under the influence of centrifugal forcing. The suspending liquid is partially wetting and is not easily amenable to spreading and instability, owing to its surface minimizing tendency. However, the suspension of neutrally buoyant hard spheres in this liquid, at increasing particle fractions (ϕ_p), exhibits greater tendency to spread before the initiation of instability compared to the spreading of the suspending liquid. Further, the wavelength of contact line instability exhibits a non-monotonic behavior within the same range of ϕ_p . The wavelength is large for $\phi_p \leq 0.4$, it decreases to a minimum in the range $0.4 < \phi_p < 0.5$ before increasing again at higher ϕ_p . The behavior at the lower and highest values of ϕ_p seems to mimic, respectively, that of a partially wetting liquid and a yield stress suspension, while the behavior at intermediate values of ϕ_p seems to mimic that of a highly wetting liquid. We explain the observed phenomena based on the predictions of linear stability analysis of the thin film equations for suspensions presented previously.^{15,16}

II. EXPERIMENTAL DETAILS

The experimental assembly shown in Fig. 1 consists of a flat, aluminium disk of diameter 15 cm driven by a computer controlled DC stepper motor. The disk can be rotated in the range 50 – 10000 revolutions per

^{a)}Current address: Pfizer, Inc., Groton, Connecticut 06340, USA.; Electronic mail: pankaj.doshi@pfizer.com

^{b)}Electronic mail: av.orpe@ncl.res.in

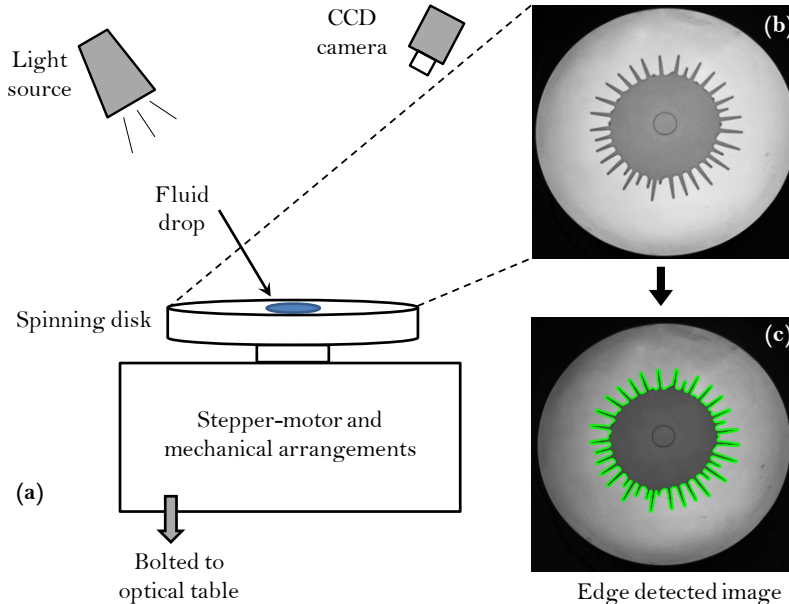


FIG. 1. Schematic of the experimental set up. (a) Spinning disk assembly and image acquisition system (b) Sample image (for PDMS) taken at certain stage of spreading (c) Same image as in (b) but superimposed with the edge detected coordinates.

minute (rpm). The desired speed is achieved from rest using an acceleration of 1000 rpm/s. The feedback controller mechanism ensures that the random fluctuations in the rotational speed are within 2% for 250 rpm while they are within 5% for 1000 rpm.

Three different fluids, two Newtonian liquids and a suspension, were used in the experiments, the properties of which are given in Table I. The suspension was prepared by immersing glass beads (of an approximate normal size distribution with mean diameter $d = 52\mu\text{m}$ and standard deviation $11\mu\text{m}$, and density 2.45 g/cc as procured from Potters, Inc.) in a liquid of matching density prepared from a mixture of LST liquid (density 2.85 g/cc) and glycerol (density 1.26 g/cc). The density matching between particles and liquid is attained to the accuracy of three decimal places. LST (Lithium heteropolytungstates) is a water soluble heavy mineral liquid, typically used for particle separations. Suspensions of varying ϕ_p (0.1 – 0.55) were prepared by mixing different amounts of glass beads in the glycerol-LST mixture. The viscosities of all the fluids, including suspensions, were obtained using the steady state rheology measurements carried out in a stress controlled rheometer. For all values of ϕ_p studied, the suspensions exhibit a Newtonian behavior for shear rates upto 10^3 s^{-1} (which are much more than those encountered in experiments) and the measured values of viscosity obey the well known Krieger-Dougherty equation for hard sphere suspensions. To measure the static contact angle, a drop of fluid was placed on the horizontal substrate. The drop was imaged by a camera placed sideways and in the plane of the substrate. The image was analyzed using ImageJ software to obtain the static contact angle. The values and corresponding errors reported in Table I represent average over 20 independent measurements.

In every experiment, a small drop of Polydimethylsiloxane (PDMS) (0.8 ml) or glycerol (1.1 ml) or suspension (1.1 ml) of particular value of ϕ_p was placed at the center of the disk. The disk surface, before every experiment, was washed multiple times using soap solution and rinsed with DI water followed by acetone to remove any traces of fluid used from the previous experiments. It was then mounted exactly horizontally on the spinning assembly. This protocol ensured the reproducibility of the experimental results. Experiments were carried out for four different rotational speeds of the disk: 250, 500, 750, and 1000 rpm. Each experiment was repeated 5 times and the results presented are averages over these experiments.

The surface of the disk is illuminated from above using a bright halogen lamp. The motion of fluid on the surface of the aluminium disk is captured from above using a high speed camera with an exposure of $150 \mu\text{s}$ to acquire sharp images. A small amount of fluorescent dye was added to the transparent fluid for ease in the fluid visualization and image analysis using better contrast (see inset of Fig. 1(b) showing a fluid, appearing in dark color, which has spread to a certain extent). The addition of the fluorescent dye changes

Fluids	Density (g cm ⁻³)	Viscosity (Pa s)	Volume (cm ³)	Static contact angle (deg)
Glycerol	1.26	0.896	1.1	68 ± 3
PDMS	0.91	0.173	0.8	7 ± 3
LST+Glycerol ($\phi_p = 0.0$)	2.45	0.022	1.1	65 ± 3
Suspension ($\phi_p = 0.100$)	2.45	0.027	1.1	65 ± 3
Suspension ($\phi_p = 0.200$)	2.45	0.043	1.1	65 ± 3
Suspension ($\phi_p = 0.300$)	2.45	0.064	1.1	65 ± 3
Suspension ($\phi_p = 0.400$)	2.45	0.096	1.1	65 ± 3
Suspension ($\phi_p = 0.425$)	2.45	0.132	1.1	65 ± 3
Suspension ($\phi_p = 0.450$)	2.45	0.162	1.1	65 ± 3
Suspension ($\phi_p = 0.475$)	2.45	0.220	1.1	65 ± 3
Suspension ($\phi_p = 0.500$)	2.45	0.295	1.1	65 ± 3
Suspension ($\phi_p = 0.525$)	2.45	0.350	1.1	65 ± 3
Suspension ($\phi_p = 0.550$)	2.45	0.763	1.1	65 ± 3

TABLE I. Physical properties of the fluids used in the experiments. The surface tensions of PDMS, Glycerol and suspending liquid (LST+glycerol) measured using pendant drop method are, respectively, 19.2 dyn cm⁻¹, 64.2 dyn cm⁻¹ and 70 dyn cm⁻¹. It is not possible to measure the surface tension of suspensions quite accurately.

the surface tensions of PDMS, glycerol, and LST-glycerol mixture by 0.05%, 0.3%, and 3.3%, respectively, which is small enough to induce any qualitative changes in the observed behavior. The acquired images were analyzed to obtain the edges of the spreading fluid using standard edge detection algorithms. The edges were detected to an accuracy of ± 0.15 mm (see Fig. 1(c)). The edge detection data were used to calculate several quantities, viz., effective radius at different radial locations (i.e., different times), spreading rates, instability wavelengths, number of fingers.

III. RESULTS AND DISCUSSION

A. Spreading behavior

Figure 2 shows the spreading of partially wetting glycerol, completely wetting PDMS and suspensions ($\phi_p = 0.45, 0.475, 0.525, 0.55$) at a rotational speed of 500 rpm. Each column corresponds to the spreading of a particular fluid at different times. Each row corresponds to the same degree of deformation of the drop boundary for all the fluids. The degree of deformation is defined as $[(R_1 - R_2)/R_2] \times 100$, where R_1 is the largest radius for the drop (distance of the farthest point from the axis of rotation) and R_2 is the radius of a circle centered on the axis of rotation and having same area as that covered by the drop. The rows 2 and 3, thus, correspond to a deformation of 10% and 20%, respectively, for all fluids.

The drop of PDMS, when placed on the disk, occupies a larger area compared to the drop of glycerol and suspensions even if the volume used is smaller (row 1 in Fig. 2). This is due to high wettability of PDMS (small contact angle) with respect to the disk surface, which spreads to occupy a larger area. The suspension drop (for all ϕ_p) occupies nearly the same area of the disk as the glycerol drop. This suggests that the suspending liquid, which has the same wettability as glycerol (nearly same contact angles as shown in Table I) primarily determines the final static configuration and the particles have relatively lesser influence. The finer details of the approach to this final static state,^{17,18} and the possible particle influence therein, are not within the scope of this work and hence was not studied.

Once the rotation of the disk is started (500 rpm as shown in Fig. 2), the drops of glycerol (first column) and PDMS (sixth column) start to spread leading towards the formation of instability along the circumference (second row) and its further growth into fingers at later times (3rd row). The radius of the base circular region of the drop at which instability first appears, does not seem to increase significantly with the fluid continuously flowing outward through the fingers which eventually reach the periphery. This overall behavior, inclusive of the instability wavelength (or number of fingers formed), is very much in accordance with the previous studies for Newtonian liquids.^{4,6}

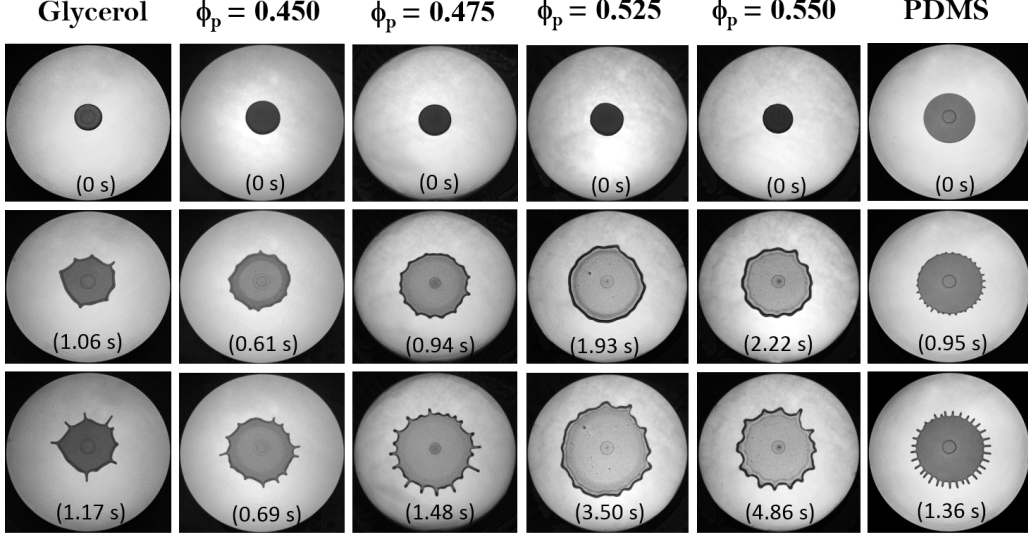


FIG. 2. Static images for a few fluids obtained at different times (or different radial positions) for a rotational speed of 500 rpm. Each column corresponds to a particular fluid while each row corresponds to the state of the fluid at a particular time (embedded in each image). The suspension images are flanked in the middle by images for partially wetting glycerol as first column and that for the completely wetting PDMS as the last column. Initial volume is 1.1 ml for all fluids except PDMS for which 0.8 ml was used.

The suspension, for all values of ϕ_p , spreads to a larger area before the instability is initiated compared to the spreading of a partially wetting liquid when the disk is rotated. Note that the suspending liquid is partially wetting, like glycerol (see relevant details in Table I). The extent of spreading, before the initiation of instability, increases gradually up to $\phi_p = 0.525$ and then decreases slightly at the highest particle fraction ($\phi_p = 0.55$). This indicates stabilization of the contact line due to the increasing presence of particles which is qualitatively similar to that observed during the spreading of a viscoelastic fluid¹⁹ and clay suspensions which exhibit a finite yield stress.^{12,15} For the values of ϕ_p studied over here, the suspensions, however, do not exhibit a yield stress or show a viscoelastic behavior as ascertained from the bulk rheology measurements. Further, when compared to pure liquids, the base circular region of suspension (for any particular ϕ_p) continues to spread significantly post the instability initiation. Increasing the rotational speed beyond 500 rpm does not qualitatively change the spreading behavior, however, lowering the rotational speed reduces the spreading tendency significantly. The qualitative behavior of the fingering instability; however, remains the same for different rotational speeds as shown later.

The time evolution of the suspension drop from its initial state up to the critical radius is shown in Fig. 3 for the rotational speed of 500 rpm along with the evolution of the drop of PDMS and glycerol. The results for the spreading/growth post-instability are shown later. The extent of spreading ($R - R_0$) is normalized by the cube root of initial volume (V_0). Here, R is the radius of the spreading drop and R_0 is the radius of the drop in its initial state. The final point in each profile corresponds to critical radius (i.e., images in the second row shown in Fig. 2). The rate of spreading of the suspension drop decreases with increase in the particle fraction which can be expected²⁰ given the increase in the viscosity (see Table I). For the highest particle fraction ($\phi_p = 0.55$) studied, the spreading rate is even lower than that observed for the two liquids. The extent of spreading ($R - R_0$) for the suspension drop, however, increases continuously with ϕ_p before decreasing slightly at $\phi_p = 0.55$. Further, the time to attain the critical radius increases monotonically with increase in ϕ_p . The overall behavior seems to arise due to combined effect of viscosity as well as the ability of a fluid to spread. For instance, the viscosities of PDMS and suspension ($\phi_p = 0.45$) are nearly the same and both possess very different static contact angles, but the extent of spreading for same degree of deformation seems to be similar. Similarly, the viscosities of glycerol and suspension ($\phi_p = 0.55$) are nearly the same and both are partially wetting (large static contact angles), but still the suspension spreads to a larger extent. Finally, the spreading rates and extent of spreading for PDMS and glycerol, which have quite different viscosities and wettabilities, are nearly the same.

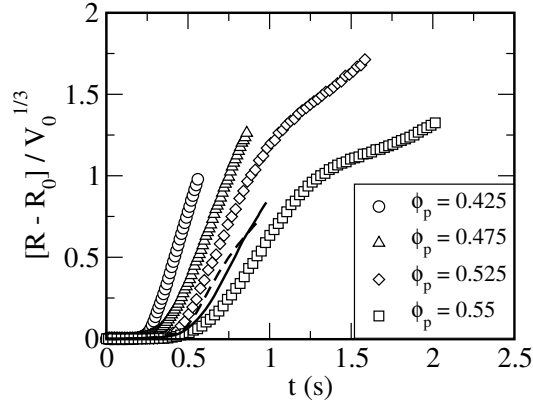


FIG. 3. Spreading of a drop from its initial position for 500 rpm. Solid line denotes the spreading of glycerol while the dashed line denotes the spreading of PDMS. The profiles represent the drop evolution from its initial position (row 1 in Fig. 2) upto the critical radius (row 2 in Fig. 2).

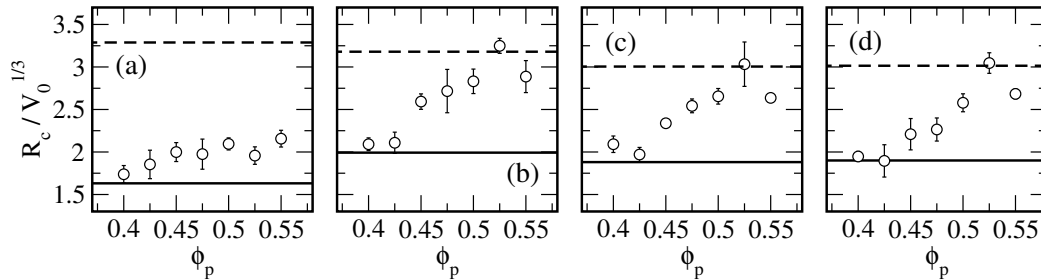


FIG. 4. Normalized critical radius (R_c) at (a) 250 rpm, (b) 500 rpm, (c) 750 rpm and (d) 1000 rpm. Open circles denote the data for suspension. Error bars denote deviations obtained by averaging over five independent data sets. Values of R_c for glycerol and PDMS are shown, respectively, as solid and dashed lines.

B. Instability and finger growth

We, now, discuss the characteristics of the contact line instability accompanying the spreading of the film. This instability ensues due to a capillary ridge region formed near the advancing front of the film, which is susceptible to perturbations in transverse direction eventually growing as fingers associated with a prescribed wavelength.²⁻⁶ The radius of the spreading film at which the instability first ensues is defined as critical radius (R_c). We measure R_c corresponding to the 10% deformation of the contact line.⁶ The value is normalized using the cube root of the initial drop volume (V_0) which is not the same for all fluids.

Figure 4 shows the variation of the normalized critical radius with ϕ_p for all the rotational speeds studied. The critical radius for PDMS decreases slightly over the range of rotational speeds employed, which is in accordance with previously observed behavior.⁶ For all other fluids, the critical radius increases with increase in rotational speed from 250 rpm to 500 rpm, beyond which it remains nearly constant. Further, the critical radius for glycerol (shown as a solid line) is much lower than PDMS (shown as a dashed line) for all the rotational speeds which is expected given that PDMS is far more wetting than glycerol and hence can spread to a larger area before developing instabilities (compare first and sixth column in Fig. 2). The value of R_c at $\phi_p = 0.4$ and lower (not shown) is quite close to that for the partially wetting glycerol for all the rotational speeds which suggests that the presence of particles has a negligible influence on the instability behavior for these values of ϕ_p . For these cases, the instability is, then, initiated due to the usual contact line instability of the partially wetting suspending liquid. Beyond $\phi_p = 0.4$, the value of R_c increases steadily (except at $\phi_p = 0.425$ for some rotational speeds which is not clear) towards that for PDMS, with a slight decrease at the highest ϕ_p for rotational speeds of 500 rpm and above. The rate of increase is smaller for 250 rpm compared to that for higher rotational speeds.

The wavelength (λ) of the instability is related to the experimentally determined critical radius (R_c) and

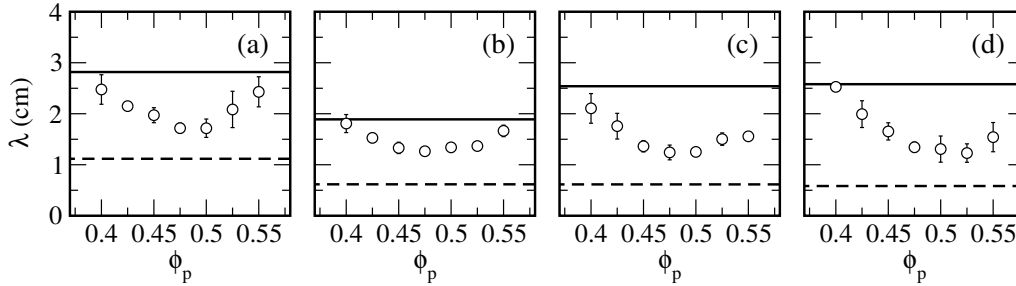


FIG. 5. Wavelength of the instability (λ) for (a) 250 rpm, (b) 500 rpm, (c) 750 rpm and (d) 1000 rpm. Open circles denote the data for suspension. Error bars denote deviations obtained by averaging over five independent data sets. Values of λ for glycerol and PDMS are shown, respectively, as solid and dashed lines.

number of ensuing fingers (N_f) as counted from the images, by the geometric relation⁶ $\lambda = (2\pi R_c)/N_f$. In Fig. 5, we show the wavelength obtained by this relation for different fluids using the experimentally determined values for R_c and the number of fingers (counted from the images) for all the four rotational speeds employed. All the measurements are carried out at a radial location where the degree of deformation is 10%. The secondary fingers which form at later times (larger degree of deformation or spreading) between the existing fingers are not included over here. PDMS has lower surface tension and breaks into several fingers associated with smaller instability wavelength. Glycerol, on the other hand, has higher surface tension and breaks into lesser fingers associated with larger instability wavelength to minimize the surface energy. This behavior is very well known in the literature and the values of the wavelength for both the liquids are in accordance with the predictions obtained through the linear stability analysis of thin film equations.^{2-4,6}

The data for suspension exhibit a very interesting non-monotonic dependence on increasing ϕ_p for all the rotational speeds. The decrease in the wavelength is in qualitative agreement with the linear stability analysis of thin film equations by Cook et al.¹⁶ These authors developed a continuum two-phase model for suspension, including concentration gradient driven diffusion and shear-induced migration of particles. This model is able to capture the decrease in the instability wavelength for a suspension film compared to that for the film of the suspending liquid. In our experiments, this raises the possibility of the presence of particle concentration gradients within the capillary ridge which can cause diffusion of particles and consequently lower wavelengths. The primary reason behind the formation of such a concentration gradient in the system, if at all present, is however not clear and needs to be investigated further. The higher wavelengths observed in Fig. 5 at higher values of ϕ_p seem to be in qualitative agreement with the predictions of linear stability analysis of thin film equations for yield stress suspension by Balmforth et al.¹⁵ The model, incorporating a Bingham stress constitutive equation, captures the increasing wavelength for a suspension film compared to the film of the suspending liquid, through the increasing yield stress. For the higher concentrations studied in our experiments, this raises the possibility of particle crowding within the capillary ridge, which will ensue a contact network and impart a yield stress, leading to the observed higher wavelengths. Again, the exact mechanism behind the crowding of the particles in the ridge, if at all present, needs further investigation.

Finally, we discuss the growth of the fingers post-instability formation. We consider only the fastest growing finger, though the behavior is more or less the same for other fingers. Figure 6 shows the growth of the fastest growing finger ($R_f - R_c$) normalized by the cube root of the initial volume (V_0) at 500 rpm. Here, R_f is the distance of the finger front from the axis of rotation and R_c is the critical radius. Glycerol forms less number of fingers and all the fluid passes outwards from the existing fingers leading to a faster growth rate (solid line in Fig. 6). In contrast, PDMS forms more fingers and the liquid flows outward through fingers as well as during the slow spreading of the central drop causing an overall lower rate in the finger growth (dashed line in Fig. 6). With increasing particle fractions, the suspension data show a monotonic decrease in the rate at which the fingers grow in time. The rate, is faster at lower values of ϕ_p , decreases and is nearly identical to that for glycerol at $\phi_p = 0.475$, decreases further to be similar to that for PDMS at $\phi_p = 0.5$ and falls further for highest values of ϕ_p studied. This overall behavior is a combination of varying viscosity and the particle influence on finger growth with increasing ϕ_p .

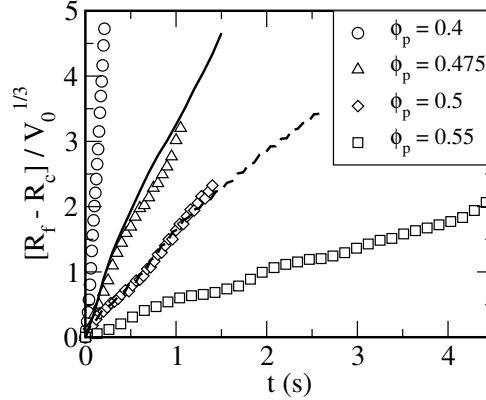


FIG. 6. Normalized growth of the fastest moving finger for 500 rpm. Solid line denotes the finger growth for glycerol while dashed line denotes the finger growth for PDMS.

IV. CONCLUSIONS

In summary, we have shown, through flow visualization experiments, a unique and curious effect of the particle fraction on the spreading behavior of a film of suspension. The critical radius for the onset of instability is found to increase gradually with increase in the particle fraction with a slight drop off at the highest particle fraction studied, while the instability wavelength decreases and then increases again while going through a minimum for the same range of particle fractions. The decrease and increase in the wavelength are, respectively, attributed to the possible particle concentration variations in the capillary ridge at lower ϕ_p and particle crowding at higher ϕ_p . The supporting arguments provided on the basis of previous theoretical studies^{15,16} are qualitative, but the results presented are, nevertheless, quite significant. They should provide strong impetus towards developing a theoretical framework capable of encompassing the existence of seemingly different spreading characteristics of a suspension film within a small concentration range. Some interesting avenues within the scope of future work are (i) actual visualization of particle motion within the capillary ridge, (ii) changes in the contact line instability for a mixture of particles differing in size, for non-neutrally buoyant particles and for non-Newtonian suspending liquids, and (iii) altering the particle surface properties to change its affinity with respect to liquid. The results also suggest possible mechanism of altering the spreading behavior of a thin film of liquid by addition of non-interacting particles which should be of interest to industrial applications.

ACKNOWLEDGMENTS

We thank Ashish Lele, Ganesh Subramaniam, Mahesh Tirumkudulu, Prabhakar Ranganathan, Prabhu Nott, and Sarika Bhattacharya for several fruitful discussions, Arun Banpurkar for providing help in measuring the surface tension of all the fluids, and Sameer Huprikar for the help provided in rheology measurements. The financial support from the Department of Science and Technology, India (Grant No. SR/S3/CE/0044/2010) is gratefully acknowledged.

- ¹A. G. Emslie, F. T. Bonner, and L. G. Peck, "Flow of a viscous liquid on a rotating disk," *J. Appl. Phys.* **29**, 858 (1958).
- ²H. E. Huppert, "Flow and instability of a viscous current down a slope," *Nature* **300**, 427 (1982).
- ³S. M. Troian, E. Herbolzheimer, S. A. Safran, and J. F. Joanny, "Fingering instabilities of driven spreading films," *Europhys. Lett.* **10**, 25 (1989).
- ⁴F. Melo, J. F. Joanny, and S. Fauve, "Fingering instability of spinning drops," *Phys. Rev. Lett.* **63**, 1958 (1989).
- ⁵M. P. Brenner, "Instability mechanism at driven contact lines," *Phys. Rev. E* **47**, 4597 (1993).
- ⁶N. Fraysse and G. M. Homsy, "An experimental study of rivulet instabilities in centrifugal spin coating of viscous newtonian and non-newtonian fluids," *Phys. Fluids* **6**, 1491 (1994).
- ⁷M. A. Spaid and G. M. Homsy, "Stability of newtonian and viscoelastic dynamic contact lines," *Phys. Fluids* **8**, 460 (1996).
- ⁸L. W. Schwartz and R. V. Roy, "Theoretical and numerical results for spin coating of viscous liquids," *Phys. Fluids* **16**, 569 (2004).
- ⁹S. Mintova and T. Bein, "Microporous films prepared by spin-coating stable colloidal suspensions of zeolites," *Adv. Mater.* **13**, 1880 (2001).

- ¹⁰M. B. Mackaplow, I. E. Zarraga, and J. F. Morris, "Rotary spray congealing of a suspension: Effect of disk speed and dispersed particle properties," *J. Microencapsulation* **23**, 793 (2006).
- ¹¹M. Pichumani, P. Bagheri, K. M. Poduska, W. González-Viñas, and A. Yethiraj, "Dynamics, crystallization and structures in colloid spin coating," *Soft Matter* **9**, 3220 (2013).
- ¹²J. R. de Bruyn, P. Habdas, and S. Kim, "Fingering instability of a sheet of yield-stress fluid," *Phys. Rev. E* **66**, 031504 (2002).
- ¹³J. Zhou, B. Dupuy, A. L. Bertozzi, and A. E. Hosoi, "Theory for shock dynamics in particle-laden thin films," *Phys. Rev. Lett.* **94**, 117803 (2005).
- ¹⁴K. E. Holloway, H. Tabuteau, and J. R. de Bruyn, "Spreading and fingering in a yield-stress fluid during spin coating," *Rheol. Acta* **49**, 245 (2010).
- ¹⁵N. Balmforth, S. Ghadge, and T. Myers, "Surface tension driven fingering of a viscoplastic film," *J. Non-Newtonian Fluid Mech.* **142**, 143 (2007).
- ¹⁶B. P. Cook, O. Alexandrov, and A. L. Bertozzi, "Linear stability of particle-laden thin films," *Eur. Phys. J. Spec. Top.* **166**, 77 (2009).
- ¹⁷J. Han and C. Kim, "Spreading of a suspension drop on a horizontal surface," *Langmuir* **28**, 2680 (2012).
- ¹⁸H. J. Jeong, W. R. Hwang, C. Kim, and S. J. Kim, "Numerical simulations of capillary spreading of a particle-laden droplet on a solid surface," *J. Mater. Process. Technol.* **210**, 297 (2010).
- ¹⁹M. A. Spaid and G. M. Homsy, "Stability of viscoelastic dynamic contact lines: An experimental study," *Phys. Fluids* **9**, 823 (1997).
- ²⁰T. Ward, C. Wey, R. Glidden, A. E. Hosoi, and A. L. Bertozzi, "Experimental study of gravitation effects in the flow of a particle-laden thin film on an inclined plane," *Phys. Fluids* **21**, 083305 (2009).